

Rationally engineered flavin-dependent oxidase reveals steric control of dioxygen reduction

Domen Zafred,^{1,2} Barbara Steiner,¹ Andrea R. Teufelberger,^{2†} Altijana Hromic,² P. Andrew Karplus,³ Christopher J. Schofield,⁴ Silvia Wallner¹ and Peter Macheroux¹

¹Institute of Biochemistry, Graz University of Technology, A-8010 Graz, Austria.

²Institute of Molecular Biosciences, University of Graz, A-8010 Graz, Austria.

³Department of Biochemistry and Biophysics, Oregon State University, Oregon 97331, U.S.A.

⁴Chemistry Research Laboratory, Department of Chemistry, University of Oxford, Oxford, OX1 3TA, United Kingdom.

[†] Present address: University Hospital Ghent, Ghent University, De Pintelaan 185, 9000 Ghent, Belgium.

Corresponding address:

Dr. Domen Zafred, Institute of Biochemistry, Graz University of Technology, Petersgasse 12, A-8010 Graz, Austria; Email: zafred.domen@gmail.com; Tel.: +43 699 1007 8283.

Article type: Original Article

Running title:

Steric control of dioxygen reduction in flavoenzymes.

Database:

Structural data are available in PDB database under the accession numbers 4PVE, 4PVH, 4PVJ, 4PVK, 4PWB, 4PWC and 4PZF.

This article has been accepted for publication and undergone full peer review but has not been through the copyediting, typesetting, pagination and proofreading process, which may lead to differences between this version and the Version of Record. Please cite this article as doi: 10.1111/febs.13212

This article is protected by copyright. All rights reserved.

Abstract

The ability of flavoenzymes to reduce dioxygen varies greatly and is controlled by the protein environment that can cause either a rapid (oxidases) or sluggish (dehydrogenases) reaction. Previously, a “gatekeeper” amino acid residue was identified that controls the reactivity to dioxygen in proteins from the vanillyl alcohol oxidase superfamily of flavoenzymes. We have identified an alternate gatekeeper residue that similarly controls dioxygen reactivity in the grass pollen allergen Phl p 4, a member of this superfamily, which has glucose dehydrogenase activity and the highest redox potential measured in a flavoenzyme. A substitution at the alternate gatekeeper site (I153V) transformed the enzyme into an efficient oxidase by increasing dioxygen reactivity by a factor of 60,000. An inverse exchange (V169I) in the structurally related berberine bridge enzyme (BBE) lowered its dioxygen reactivity by a factor of 500. Structural and biochemical characterization of these and additional variants showed that our model enzymes have a cavity binding an anion and resembling the “oxyanion hole” in the proximity of the flavin ring. We showed also that steric control of access to this site is the most important parameter affecting dioxygen reactivity in BBE-like enzymes. Analysis of flavin-dependent oxidases from other superfamilies revealed similar structural features suggesting that dioxygen reactivity might be governed by a common mechanistic principle.

Introduction

Flavin dependent enzymes catalyze redox reactions ranging from oxidations of alcohols, aldehydes, and amines, to monooxygenation, halogenation, complex bond formation and cyclization reactions [1–3]. Flavoenzymes that employ dioxygen as an electron acceptor can function as oxidases, reducing oxygen to hydrogen peroxide, or as monooxygenases, splitting the molecule such that one oxygen atom is incorporated into a hydroxylated product, and the other into water. Kinetically, the transfer of the first electron to dioxygen appears to be the rate-limiting step in the process (Fig. 1) and while free reduced flavin in solution reacts relatively slowly with dioxygen, flavin-bound proteins can decelerate or accelerate this reaction substantially, spreading its rate over six orders of magnitude [4,5].

A flavin-(4a)-hydroperoxide adduct has been characterized in FAD-dependent monooxygenases [6] and recent studies of dioxygen activation have shed light on the mechanism of dioxygen utilization in these enzymes [7,8]. Based on the occurrence of the flavin-(4a)-adduct, the reactive carbon atom has been accepted as the site of electron transfer in reaction with dioxygen in flavoenzymes, however, the resulting hydroperoxide intermediate has never been observed in flavin dependent oxidases (Fig. 1) [5,9]. While the recent characterizations of single atom adducts suggested that the flavin-(4a)-hydroperoxy adduct is a likely intermediate in some flavin dependent oxidases [10,11], there is evidence that the reaction might also proceed without formation of this adduct [12,13].

In recent years several studies have provided insights into the specific roles of certain residues in flavoenzymes. Model proteins have been used to identify putative oxygen channels, influences of substrate and inhibitor binding and altered flavin redox potentials [5,9,14]. Active site residues, such as histidine H516 in the proximity of FAD in glucose oxidase (**PDB ID: 1GPE**) [15] or the conserved lysine in the proximity of N(5) in fructosamine oxidase (**PDB ID: 3DJE**) and monomeric sarcosine oxidase (**PDB ID: 1L9E**) have suggested an important role of a positively charged amino acid residue to regulate the dioxygen reactivity of reduced flavins

This article is protected by copyright. All rights reserved.

[16–18]. Despite this progress it is still questionable whether there is a common catalytic principle that governs the reactivity of the reduced flavin toward dioxygen.

The vanillyl alcohol oxidase (VAO) structural superfamily (also called the *p*-methylcresolhydroxylase [PCMH] structural superfamily) includes FAD dependent hydroxylases, oxidases and dehydrogenases, most of which employ a mono- or bicovalently bound cofactor [19,20]. These enzymes have a two-domain structure with the cofactor buried in the FAD binding domain and the redox-active isoalloxazine ring oriented with its *si*-face towards the active site cavity where substrate binding is organized by the substrate binding domain [21,22]. The *re*-face of the FAD is surrounded by a conserved 18-residue long segment of chain that we will refer to as the “oxygen reactivity motif” and which creates the environment of the isoalloxazine ring above the C(4a) reactive carbon atom. This motif contains what was described by Leferink et al. [23] as the “gatekeeper” residue at a position suitable for the control of dioxygen reactivity in the VAO superfamily. In their model enzyme L-galactono- γ -lactone dehydrogenase (GALDH), replacement of a gatekeeper alanine with glycine (A113G) increased oxygen reactivity 400-fold. The correlation in the VAO superfamily was not perfect as seven of the 30 oxidases listed in their study (see their supplementary Table 1) had an alanine or a proline at the gatekeeper position, suggesting that additional complexities exist in defining oxidase activity in the superfamily.

In the present study, we have further investigated the control of oxygen reactivity in the VAO superfamily by employing the berberine bridge enzyme (BBE, EC 1.21.3.3) and the BBE-like protein pollen allergen Phl p 4 as models. BBE-like enzymes are a subgroup of PCMH/VAO superfamily, classified as pfam08031 (superfamily cl06869) in the Conserved Domain Database [24]. BBE from the California poppy catalyzes the oxidative cyclization of (*S*)-reticuline to (*S*)-scoulerine by formation of a carbon-carbon bond, the berberine bridge [25]. Phl p 4 from Timothy grass shows extensive similarity to BBE (34% sequence identity), has a similar overall topology (RMSD of aligned C α atoms is 1.53 Å) and a conserved bicovalent linkage of the FAD [22]. Despite these structural similarities, Phl p 4 does not catalyze C-C bond formation, but instead oxidizes D-glucose. In contrast to BBE and other previously characterized BBE-like enzymes, reduced Phl p 4 reacts sluggishly with dioxygen suggesting that the FAD cofactor is reoxidized by an alternative electron acceptor *in vivo*. In other words, Phl p 4 behaves like a dehydrogenase rather than an oxidase, despite having a glycine at the gatekeeper position. Since this is a feature common to all known BBE-like enzymes [26], the gatekeeper identified by Leferink et al. does not explain suppressed oxygen reactivity of Phl p 4 and we sought to find a novel structural feature.

Closer inspection of the active sites of BBE and Phl p 4 revealed that while the position of FAD and the topology of the protein backbone are highly conserved, this is not the case for several amino acid side chains near the isoalloxazine ring, such as H459/Y439 on the *si*-face or H174/N158 and V169/I153 on the *re*-face of BBE and Phl p 4, respectively (Fig. 2A). The backbone nitrogen of cysteine C166/C150 (the residue covalently attached at the flavin C6 position) is in a loop above the *re*-face of the flavin in BBE-like enzymes and too far away to interact with the isoalloxazine ring or any protein residue (*e.g.* by formation of a hydrogen bond, Fig. 2). In contrast, the backbone nitrogen of the preceding W165/V149 is within hydrogen bond distance to the C(4)=O carbonyl group. These two residues are oriented towards the *re*-face of the flavin and placed adjacent to a small cavity that is positioned above the C(4a) carbon atom and lined by the side chains of V169, H174 and L145 in BBE (Fig. 2). This small cavity, with nearby partial positively charged backbone nitrogens available for hydrogen

This article is protected by copyright. All rights reserved.

bonding, is reminiscent of the “oxyanion hole” observed in certain hydrolases [27] and potentially able to bind oxygen in BBE-like oxidases. In this paper, we will call it “oxygen pocket”, a term that was introduced by Lindqvist et al. for a similar structural feature described in glycolate oxidase [28]. Interestingly, the oxygen pocket does not exist in Phl p 4 because the C δ methyl group of I153 projects towards the C(4a) and fills the cavity (Fig. 2B).

Based on these considerations, we created a set of BBE (G164A, V169I and G164A V169I) and Phl p 4 variants (I153V, N158H and I153V N158H) to investigate the role of the side chains involved in shaping of the oxygen pocket formed by the oxygen reactivity motif on the *re*-face of the isoalloxazine ring. The Phl p 4 I153V variant had a remarkable 60,000-fold higher dioxygen reactivity compared to the wildtype enzyme, leading us to identify this position as an alternate gatekeeper residue that is crucial for the control of oxygen reactivity in BBE-like enzymes. These results not only make it possible to predict oxygen reactivity of members of the BBE-like enzyme family, but as we discuss, they also have implications for other flavoenzyme families that appear to have an analogous oxygen pocket in the proximity of the reactive C(4a).

Results

Biochemical characterization of the BBE and Phl p 4 variants

All BBE and Phl p 4 variants were successfully expressed in *Komagataella pastoris* (formerly *Pichia pastoris*) and purified to homogeneity as described in Experimental Procedures. While BBE variants, wildtype Phl p 4 and Phl p 4 N158H were stable over longer periods of time, changes in the UV/Vis absorption spectrum of the Phl p 4 I153V single and I153V N158H double variant indicated the slow formation of spirohydantoin during purification and storage [29].

Kinetic parameters were determined for BBE as well as Phl p 4 variants and a summary of the oxidative and reductive rates is given in Table 1. In the case of BBE, the single variants showed a similar (G164A) and five-fold lower (V169I) rate constant for the reduction by its substrate (*S*)-reticuline. In contrast, the rate of reoxidation of the reduced variants by dioxygen dropped by 500 to 1000-fold, from $\sim 50,000$ to ~ 50 M $^{-1}$ s $^{-1}$, and were not further decreased in the double variant (Table 1).

Wildtype Phl p 4 and its three variants showed similar reactivity with glucose (Table 1) and no saturation was observed even at 10 mM glucose. In contrast to BBE, reduced wildtype Phl p 4 reacts with dioxygen at a rate of 1.2 M $^{-1}$ s $^{-1}$, more than two orders of magnitude below that of free FAD (250 M $^{-1}$ s $^{-1}$). The N158H variant showed a similar rate of reoxidation, however, both the single I153V and the I153V N158H double variant exhibited much higher rates of reoxidation, with 7.1 and 3.9 x 10 4 M $^{-1}$ s $^{-1}$, respectively. Thus it is evident that residue I153 plays a major role in controlling dioxygen reactivity in Phl p 4 and the I153V variant very effectively converted this dehydrogenase into an oxidase by elevating its dioxygen reactivity more than four orders of magnitude (Table 1).

Bivalent modification of the isoalloxazine ring contributes to the positive redox potential found in BBE and other flavoproteins of the VAO superfamily [25,30], and because this can play a role in reactivity, we measured the redox potentials of the various enzyme forms. The three BBE variants exhibited redox potentials

of approximately +110 mV, which is comparable to wildtype enzyme ($E_0 = 132$ mV, Table 1). Wildtype Phl p 4 and its variants had redox potentials in the range of +200 mV, approaching the O_2/H_2O_2 redox couple (270 mV), and roughly 400 mV more positive than that of free FAD (Fig. 3, Table 1).

Structural features of the variants and crystallographic experiments with surrogates

Intrigued by the strong effects of the V169I and G164A exchanges in BBE and the I153V substitution in Phl p 4, we solved a set of crystal structures at 1.3 to 2.3 Å resolution (Table 2) to gain insight into the structural changes that tune the properties of the variants. Overall, the structures determined for Phl p 4 variants were virtually superimposable with the respective wildtype structure and no structural perturbations were observed. The I153V exchange in Phl p 4 creates space at the *re*-face of the isoalloxazine ring, resulting in formation of a pocket similar to that in wildtype BBE. In the latter, the oxygen pocket is removed by replacement of the glycine in the gatekeeper position with an alanine, *i.e.* G164A, where C β of the alanine side chain protrudes towards the FAD and pushes the isoalloxazine ring slightly in the direction of the *si*-face (Fig. 2B). While the structure of the BBE V169I mutant was not determined, it is reasonable to expect that the extra methyl group would fill the cavity analogously to the wildtype Phl p 4. Thus it appears that the key structural difference between wildtype BBE and Phl p 4 involved in control of oxygen reactivity concerns the existence of the oxygen pocket placed in the proximity of the reactive C(4a) carbon atom (Fig. 2).

Xenon pressurization experiments with crystals of Phl p 4 I153V yielded a structure with two xenon atoms placed in hydrophobic pockets of the FAD binding domain, but not in the proximity of the isoalloxazine ring (Table 2, Fig. 4A). It has been shown for other flavoproteins oxidases that halide ions can be used as a surrogate for locating putative oxygen binding sites [31] and when halide ions were used in our crystal soaking experiments, an ion at low occupancy was observed in the engineered oxygen pocket of both Phl p 4 variants (I153V and I153V N158H), with the best results being obtained for sodium bromide and the Phl p 4 I153V N158H (Table 2, Fig. 4). The presence of the halide ion at the site was confirmed by an anomalous difference map and the ion was fitted into the $F_o - F_c$ difference density. This anion bound in the oxygen pocket is positioned ~ 2.5 Å above the C(4a) atom on the *re*-face, and ~ 3.6 Å away from the C γ -methyl of V153 (Fig. 4B). The ion is stabilized by the backbone amide nitrogens of C150 and V149 at a distance of approximately 3.4 Å. Superposition of this structure with the structure of wildtype Phl p 4 highlights that ion binding is not feasible in the wildtype enzyme due to a clash with C δ atom of I153 (Fig. 4B).

Dioxygen reaction mechanism and putative transition states

FAD in all our Phl p 4 structures adopted a butterfly bent shape [22], resembling reduced FAD that is bent due to sp^3 hybridization of the N5 and N10 atoms in the central pyrazine ring. The putative intermediate in the reaction of reduced FAD with dioxygen is expected to be further twisted due to sp^3 hybridization of the carbon in the C(4a) position, but the shape of the bent isoalloxazine ring derivative can vary significantly. To gain a sense for what structures can be modeled in the active sites of our Phl p 4 and BBE variants, we have compared four flavin derivatives (Fig. 5). The distal oxygen atom of the peroxy adduct in our models was positioned analogously to the position of C(18) in 4a,5-epoxyethano-3-methyl-4a,5-dihydrolumiflavin (Emmdh-flavin).

When models of flavin-4a-hydroperoxides with the peroxy group protruding on the *re*-face are aligned with the structure of Phl p 4 I153V N158H, the adduct fits into the oxygen pocket but C(4)=O clashes with the side chain of Y439 in all models except when Emmdh-flavin is used (Fig. 6B). No clashes are observed when derivatives are modeled in the structure of wildtype BBE (data not shown). When alignments with the peroxy adduct at the *si*-face are performed, the C(4)=O atom fits into the oxygen pocket (Fig. 6A).

Discussion

BBE has been studied extensively and while several variants of amino acid exchange in the active site have been created to identify the residues involved in substrate binding and catalysis, none of these replacements had a significant effect on the oxidative half reaction with dioxygen (Table 3) [25,29,32,33]. The substitutions previously studied in BBE include residues implicated as important by corresponding studies with other flavoenzymes [9,17]. Although (at least partial) positive charge in close proximity of the FAD was eliminated in the H459A, H174A and H104A BBE variants, the dioxygen reactivity was hardly affected. Moreover, removing hydrogen bond donors in the proximity of N(10) on the *si*-face of the isoalloxazine ring in Y106F and H459A BBE variants did not show a substantial effect on the rate of flavin reoxidation (Table 3). In the present study, a new set of BBE and Phl p 4 variants was generated and characterized with the aim to identify amino acids responsible for the control of dioxygen reactivity in the VAO superfamily.

Reciprocal single amino acid substitutions at the *re*-face of the FAD were created to study the effect on the oxidative half reaction of the reduced enzyme with dioxygen by incorporating BBE-derived amino acid residues in Phl p 4 and *vice versa* (Table 1, Fig. 2 and Fig. 4). In the case of Phl p 4, substitution of the “alternate gatekeeper” residue isoleucine I153 to valine prompted a 60,000-fold increase in the rate of oxidation while the inverse amino acid exchange in BBE V169I resulted in a less pronounced but still substantial 500-fold decrease in oxygen reactivity (Table 1). Introduction of an alanine at the “gatekeeper” position of BBE (G164A) had a slightly stronger effect on dioxygen reactivity and introduction of both mutations did not further suppress the reaction (Table 1). Even though the decline in oxygen reactivity of the BBE variants was smaller, the attained level of reactivity is considerably lower than the reactivity of free reduced FAD (Table 1). The redox potentials of the enzyme-bound FAD were not substantially affected by the amino acid substitutions in any of the variants (Table 1), proving that redox potential has no effect on oxygen reactivity even in Phl p 4, a protein that exhibits the highest redox potential ever measured in a flavin dependent enzyme.

X-ray crystal structure analysis enabled us to show that the only considerable difference between the oxygen reactive and non-reactive variants is the existence of the “oxygen pocket” formed by the “oxygen reactivity motif” with two backbone amide nitrogens pointing towards the *re*-face of the FAD above the reactive C(4a) (Fig. 4). This cavity can be removed by introduction of a single methyl group on either side: frontal above the C(4)=O where the gatekeeper resides at a conserved position or on the opposite side of the cavity where the Phl p 4 derived alternate gatekeeper resides in some VAO sub-families, including the BBE-like enzymes. In the case of BBE, valine in this position allows access to the oxygen pocket whereas the additional methyl group of isoleucine causes steric hindrance in Phl p 4 (Fig. 2 and 4). We conclude that the observed effects on the oxidative rates were caused exclusively by changes in the accessibility of the backbone amide nitrogens of W165/V149 and C166/C150 and the *re*-face of the FAD. The existence of the partial positive charge in the cavity

was supported by our halide soaking experiments, which showed that even though tightly packed, a halide ion can be bound in the oxygen pocket while xenon atom can not (Fig. 4). As shown before, xenon readily binds in hydrophobic pockets and thus putative dioxygen binding sites, but not at dioxygen reaction sites [34,31]. A similar halide binding site was previously seen in the VAO crystal structure (Fig. 7) and was suggested to represent the dioxygen binding site [5,35].

Interestingly, the complete environment at the *re*-face of FAD is defined by the oxygen reactivity motif in VAO superfamily enzymes. While the gatekeeper residue and position of the neighboring amide nitrogen are conserved among all VAO superfamily enzymes, the rest of the motif varies significantly (Fig. 7). For instance, in VAO there is no alternate gatekeeper residue that could be aligned with the I153 of Phl p 4 (Fig. 7). Another example is alditol oxidase (AldO, **PDB ID: 2VFR**), which is an oxidase even though it has alanine A105 at the gatekeeper position and isoleucine I110 at the alternate gatekeeper position. It is a backbone shift of the oxygen reactivity motif that moves the gatekeepers away from the reactive C(4a) in this enzyme (Table 4, Fig. 7) [36].

While universal predictions do not extend to all members of the VAO superfamily, reliable predictions are possible within sub-families having members with solved representative structures. For example, BBE-like enzymes, which are abundant in the plant kingdom (the model plant *Arabidopsis thaliana* contains 28 genes encoding BBE-like enzymes [26]), have an invariant glycine at the gatekeeper position, while the residue at the Phl p 4 derived alternate gatekeeper position is either a valine, leucine or isoleucine, suggesting that oxidases and dehydrogenases are present.

Towards a unifying concept of dioxygen reactivity in flavoenzymes

Since our study revealed that access to the oxygen pocket in flavoenzymes of the VAO superfamily is essential for dioxygen reactivity, we explored whether equivalent structural parameters exist in other flavoenzyme superfamilies. Interestingly, the existence and role of an analogous structural feature in dioxygen reactivity was already discussed for *p*-hydroxybenzoate hydroxylase (PHBH, **PDB ID: 1PHH**) more than two decades ago by Schreuder and coworkers [37]. These authors realized that the structure of Emmdh-flavin [38] fits perfectly into the active site of PHBH with the C(4)=O gaining two strong hydrogen bonds upon moving into a hole formed by two backbone nitrogens, which they termed “carbonyl oxygen binding pocket”. They stressed that the binding pocket strongly resembles the oxyanion hole, at a time already known as a key feature of various proteases. PHBH is a member of the glucose–methanol–choline oxidoreductase (GMC) family, which includes other well-studied flavoenzymes such as choline oxidase, glucose oxidase and D-amino acid oxidase [10,39,40]. In contrast to the VAO superfamily, the organic substrate binds on the *re*-face of the flavin and the oxygen pocket is on the *si*-face, making these functional similarities an interesting case of convergent evolution (Fig. 8).

A few years later a cavity termed the “oxygen pocket” was described by Lindqvist et al. who studied structural features of FMN dependent glycolate oxidase (**PDB ID: 1GOX** and **1AL7**). The protein was compared to flavocytochrome b2, a dehydrogenase in which the proton donor is absent due to a backbone shift (**PDB ID: 1FCB**) [28]. This pocket resides at the *re*-face of the FMN and is filled with a water molecule in the native structure of glycolate oxidase (Fig. 8). Unlike in VAO and GMC oxidoreductases where two amide groups serve as

the proton donors, the oxygen pocket of glycolate oxidase is formed by a serine S106 side chain positioned at a hydrogen bond distance from the backbone oxygen of T78 and a side chain of glutamine Q127 (Fig. 8).

We find similar structural patterns also in flavin dependent oxidases from other structural superfamilies where structural features analogous to the oxygen pocket have not been previously discussed. Enzymes of the acyl-CoA oxidase family exhibit two backbone nitrogen atoms at the *si*-face of the FAD, at a distance that would allow for strong hydrogen bonding upon movement of the C(4)=O, analogous to that proposed for PHBH (Fig. 8) [41]. In the case of fructosamine oxidase and monomeric sarcosine oxidase, replacement of a conserved lysine in the active site removes a strongly bound water molecule in the proximity of the N(5) atom [17,18,42]. In light of the assumed importance of the oxygen pocket, we suggest that this water molecule, together with the adjacent backbone nitrogen of V105, could be involved in formation of the oxygen pocket (Fig. 8).

These examples illustrate that the concept of an “oxygen pocket” might be generally applicable to flavoenzyme oxidases, albeit with a great deal of variation in the structural organization that depends on how the isoalloxazine ring is embedded into the protein matrix.

Possible mechanisms of dioxygen reactivity

Dioxygen reaction with free reduced flavin does not distinguish between the sides of the isoalloxazine ring, however, in enzymes this is not the case as the protein matrix renders the *re*- and *si*-face asymmetric. We assume that oxygen reaction occurs at the C(4a) carbon in our model enzymes [4,9], but our experiments do not allow us to distinguish a radical reaction from the reaction with a hydroperoxy intermediate (Fig. 1).

Nonetheless, we believe that conformation, orientation and spatial arrangement of radicals in case of the radical reaction would be similar to the covalent derivatives. Since C(4a) peroxy flavin derivatives have been observed in flavin dependent monooxygenases and are likely intermediates in certain oxidases [9], we have built models with FAD derivatives, the putative reaction intermediates occurring during the proposed reoxidation reaction (Fig. 1). Our models were based on four structures of flavin derivatives, three of which were found in proteins (Fig. 5). Large variation of movements of carbonyl C(4)=O out of the plane upon C(4a) sp^3 hybridization can be observed in these derivatives, apparently due to the protein environment. We were able to align these models in the active sites of our proteins with confidence, because the flavin ring is firmly anchored within the protein matrix and is severely restricted in its movement in BBE-like proteins due to the covalent bonds to the cysteine and histidine side chains in combination with a strongly bound ribityl moiety.

According to our modeling, major movements of the C(4)=O carbonyl group out of the plane and into the oxygen pocket, occurring upon oxygen adduct formation at the *si*-face, are only possible in oxidase variants (Fig. 6). In the non-reactive variants alanine at the gatekeeper position as well as isoleucine in the position of the alternate gatekeeper prevent movements of the carbonyl oxygen towards the proton donors. Similarly, adduct formation is sterically possible on either side of the ring in our oxidase variants, but only on the *si*-face in the non-reactive variants. Therefore two scenarios are sterically possible where an accessible oxygen pocket could play a major role in dioxygen reactivity in our model proteins; either the pocket stabilizes the peroxy adduct directly on the *re*-face of FAD, or, if dioxygen attack occurs from the *si*-face, it stabilizes the C(4)=O carbonyl oxygen in its twisted conformation (Fig. 6).

It is worth pointing out that the two reaction options in BBE-like enzymes may not be mutually exclusive and theoretically both could be taking place in certain members of the superfamily, while in some cases, such as enzymes of the acyl-CoA dehydrogenase or GMC superfamily, only one reaction mode is sterically feasible. Also, it is important to stress that both discussed reaction paths provide a rationale of how the sp^3 hybridized transition state is stabilized during the reoxidation of the reduced flavin and thus rationalize a fundamental principle of enzyme catalysis.

Conclusion

In this study we have achieved substantial changes in the oxygen reactivity of flavin-dependent enzymes based on a rational design of active site residues by mutagenesis. Our combined biochemical analysis and structural results reveal that hydrophobic residues in the proximity to the isoalloxazine ring govern dioxygen reaction by controlling the access to the oxygen pocket, a feature that strongly resembles the oxyanion hole. In addition, we have demonstrated that these structural features enable the prediction and manipulation of dioxygen reactivity in BBE-like enzymes. The conservation of the oxygen pocket in the VAO/PCMH superfamily suggests that amino acid replacements with equivalent structural impact will have similar effects on the oxygen reactivity of other members, however, reliable predictions of dioxygen reactivity that are based solely on sequence alignment are only possible within subgroups of structurally highly related proteins. Furthermore, exploration of the structures of flavin-dependent oxidases from other superfamilies indicates that dioxygen reactivity might be governed by similar principles, *i. e.* the occurrence of and access to an oxygen pocket in the proximity of the reactive C(4a) carbon atom.

Experimental Procedures

Reagents

Chemicals were purchased from Sigma-Aldrich and oligonucleotide primers were ordered from VBC-Biotech. (*S*)-reticuline was from the natural product collection of the Donald Danforth Plant Science Center (St. Louis, U.S.A.) and (*rac*)-reticuline was synthesized as described [43].

Cloning, expression and purification

Mutagenesis was performed to create the [pPICZ α - BBE V169I], [pPICZ α - BBE G164A], and [pPICZ α - BBE G164A V169I] expression plasmids using the QuikChange[®] XL Site-Directed Mutagenesis Kit (Stratagene). As a template for the polymerase chain reaction, the expression vector [pPICZ α BBE-ER] was used as described before [44]. Non-glycosylated Phl p 4.0202 was used in this study (**UniProt Protein Database ID: B2ZWE9**). Genes of all Phl p 4 variants were ordered from GenScript and cloned into pPICZ α vector (Invitrogen).

Expression plasmids were transformed using electroporation into the expression strain *Komagataella pastoris* (formerly *Pichia pastoris*) KM71H coexpressing the *S. cerevisiae* protein disulfide isomerase. Integration of the expression cassettes into the *Komagataella* genome was verified using colony polymerase chain reaction. Protein production was carried out in a BBI CT5-2 fermenter (Sartorius) as described previously [43] and stopped. This article is protected by copyright. All rights reserved.

after 100-150 h of methanol induction. Purification of BBE variants was performed as described [43] and purification of Phl p 4 was done by an adopted protocol from Nandy et al. [45].

Transient Kinetics

Reductive and oxidative half-reactions were analyzed with a stopped-flow device (SF-61DX2, Hi-Tech) at 25°C in an anaerobic atmosphere provided within a glove box (Belle Technology). All samples were rendered oxygen-free by flushing with nitrogen and subsequent incubation in the glove box. Spectral changes of the flavin cofactor were followed using a KinetaScanT diode array detector (model MG-6560, Hi-Tech).

Reductive half-reaction: In BBE variants rate constants were determined in 100 mM Tris-HCl, pH 9.0 at substrate concentrations from 30 to 500 μ M (*S*)-reticuline. Apparent rate constants were plotted against the respective substrate concentrations and fitting the resulting data with a non-linear hyperbolic curve led to determination of the reductive rate constant k_{red} . Measurements of Phl p 4 variants were performed in 80 mM KH_2PO_4 , pH 6.7, with 100 mM NaCl, using 5 μ M to 100 mM final D-glucose concentrations. Fitting of obtained transients at 450 nm was performed with Kinetic Studio Software (TgK Scientific).

Oxidative half-reaction: Rates were determined by mixing air-saturated buffers with an oxygen free substrate-reduced enzyme solution. Reduction of the FAD cofactor was performed with substoichiometric amounts of (*rac*)-reticuline or glucose in order to prevent lag-phases in the reoxidation process.

Redox Potential Determination

Redox potentials were determined at 25 °C by an adapted method from Olson et al. [46]. Experiments with BBE variants were performed in 50 mM potassium phosphate buffer, pH 7.0, while Phl p 4 variants were measured in 50 mM HEPES, pH 7.0. All experiments were carried out in a glove box as described above. Toluylene blue ($E_0=115$ mV) was used as redox dye for redox potential determination of BBE and dichlorophenolindophenol (DCPIP, $E_0=217$ mV) for Phl p 4. The standard protein potentials were calculated from plotted Nernst equation according to Minnaert [47].

Crystallization, data collection and structural characterization

BBE G164A was crystallized in batch, mixing protein (35 mg/mL in 20 mM Tris, pH 7.0) in 1:1 ratio with crystallization buffer (100 mM HEPES, pH 7.5, 2.0 M ammonium sulfate). Phl p 4 variants were crystallized using the sitting drop method, mixing protein (7 mg/mL in 20 mM Tris pH 7.0) in 3:2 ratio with crystallization buffer (70% Tacsimate, pH 7.0), 43% PEG 2000 was used as the reservoir solution. All crystals were soaked in a solution composed of crystallization buffer with 20% glycerol and frozen in liquid nitrogen. To obtain the crystal structure with bromide, crystals were soaked in crystallization solution with 20% glycerol and 3.5 M sodium bromide prior to freezing [34,31]. To obtain the structure with xenon, crystals were soaked in crystallization solution with 20% glycerol and pressurized at 40 bar of xenon in a home-built device (details will be described elsewhere). The crystal was frozen instantly after pressure was released. Data sets were collected at beam lines FIP-BM30A, ID29 and ID23-1 (ESRF, Grenoble), I04-1 (Diamond, Didcot) and P11 (Petra III, Hamburg). Data were processed with

This article is protected by copyright. All rights reserved.

XDS [48], molecular replacement was conducted with Phaser [49] and structures were refined with Phenix [50] and Coot [51]. Structures of wildtype Phl p 4 and variants have a positive electron density in the active site at the *si*-face of the FAD that varies in size and shape. It is probably derived from ingredients of crystallization buffer, glycerol and protein impurities (like the sulfite adduct) therefore we have decided to leave it empty in deposited structures. Proteins were superimposed in PyMol by aligning three FAD atoms: C(6), C(8) and N(10). Models of peroxy adducts are based on the structure of 4a,5-epoxyethano-3-methyl-4a,5-dihydroflavin [38]. Models as well as figures were prepared with PyMol (Schroedinger) and finished with Gimp.

Acknowledgements

This research was supported by the “Fonds zur Förderung der wissenschaftlichen Forschung” (FWF) through SFB projects F1805 and F4604 and by the PhD program “Molecular Enzymology” (W901). A short-term visit of D. Zafred to the laboratory of Prof. C. J. Schofield was supported by EMBO. We are grateful to Prof. Walter Keller for his financial support and resourceful discussions. We would like to thank Drs. Andrea Camattari, Jean-Luc Ferrer, Frank von Delft and Michael McDonough for their support and technical help with experiments.

Author contributions

S.W., B.S., A.H. expressed, purified and enzymatically characterized BBE variants. D.Z., S.W., A.R.T. expressed, purified and enzymatically characterized Phl p 4 variants. D.Z. designed research, crystallized and structurally characterized proteins, prepared figures. Manuscript was written by D.Z., P.M., S.W., P.A.K., C.J.S.

References

- 1 Fagan RL & Palfey BA (2010) Flavin-dependent enzymes. In *Comprehensive Natural Products II* (Begley TP, ed), 7th ed., pp. 37–114. Elsevier, Amsterdam.
- 2 Teufel R, Miyanaga A, Michaudel Q, Stull F, Louie G, Noel JP, Baran PS, Palfey B & Moore BS (2013) Flavin-mediated dual oxidation controls an enzymatic Favorskii-type rearrangement. *Nature* **503**, 552–556.
- 3 Liu Y-C, Li Y-S, Lyu S-Y, Hsu L-J, Chen Y-H, Huang Y-T, Chan H-C, Huang C-J, Chen G-H, Chou C-C, Tsai M-D & Li T-L (2011) Interception of teicoplanin oxidation intermediates yields new antimicrobial scaffolds. *Nat. Chem. Biol.* **7**, 304–9.
- 4 Massey V (1994) Activation of molecular oxygen by flavins and flavoprotein. *J. Biol. Chem.* **269**, 22459–22462.
- 5 Mattevi A (2006) To be or not to be an oxidase: challenging the oxygen reactivity of flavoenzymes. *Trends Biochem. Sci.* **31**, 276–83.

This article is protected by copyright. All rights reserved.

- 6 Vervoort J, Muller F, Lee J, van den Berg WAM & Moonen CTW (1986) Identifications of the true carbon-13 nuclear magnetic resonance spectrum of the stable intermediate II in bacterial luciferase. *Biochemistry* **25**, 8062–8067.
- 7 Orru R, Dudek HM, Martinoli C, Torres Pazmiño DE, Royant A, Weik M, Fraaije MW & Mattevi A (2011) Snapshots of enzymatic Baeyer-Villiger catalysis: oxygen activation and intermediate stabilization. *J. Biol. Chem.* **286**, 29284–91.
- 8 Thotsaporn K, Chenprakhon P, Sucharitakul J, Mattevi A & Chaiyen P (2011) Stabilization of C4a-hydroperoxyflavin in a two-component flavin-dependent monooxygenase is achieved through interactions at flavin N5 and C4a atoms. *J. Biol. Chem.* **286**, 28170–80.
- 9 Chaiyen P, Fraaije MW & Mattevi A (2012) The enigmatic reaction of flavins with oxygen. *Trends Biochem. Sci.* **37**, 373–80.
- 10 Orville AM, Lountos GT, Finnegan S, Gadda G & Prabhakar R (2009) Crystallographic, spectroscopic, and computational analysis of a flavin C4a-oxygen adduct in choline oxidase. *Biochemistry* **48**, 720–728.
- 11 Tan TC, Spadiut O, Wongnate T, Sucharitakul J, Krondorfer I, Sygmund C, Haltrich D, Chaiyen P, Peterbauer CK & Divne C (2013) The 1.6 Å crystal structure of pyranose dehydrogenase from *Agaricus meleagris* rationalizes substrate specificity and reveals a flavin intermediate. *PLoS One* **8**, e53567.
- 12 Pennati A & Gadda G (2011) Stabilization of an intermediate in the oxidative half-reaction of human liver glycolate oxidase. *Biochemistry* **50**, 1–3.
- 13 Gannavaram S & Gadda G (2013) Relative timing of hydrogen and proton transfers in the reaction of flavin oxidation catalyzed by choline oxidase. *Biochemistry* **52**, 1221–6.
- 14 Baron R, Riley C, Chenprakhon P, Thotsaporn K, Winter RT, Alfieri A, Forneris F, van Berkel WJH, Chaiyen P, Fraaije MW, Mattevi A & McCammon JA (2009) Multiple pathways guide oxygen diffusion into flavoenzyme active sites. *Proc. Natl. Acad. Sci. U. S. A.* **106**, 10603–8.
- 15 Klinman JP (2007) How do enzymes activate oxygen without inactivating themselves? *Acc. Chem. Res.* **40**, 325–33.
- 16 Gadda G (2012) Oxygen activation in flavoprotein oxidases: the importance of being positive. *Biochemistry* **51**, 2662–9.
- 17 McDonald CA, Fagan RL, Collard F, Monnier VM & Palfey BA (2011) Oxygen reactivity in flavoenzymes: context matters. *J. Am. Chem. Soc.* **133**, 16809–11.
- 18 Zhao G, Bruckner RC & Jorns MS (2008) Identification of the oxygen activation site in monomeric sarcosine oxidase: role of Lys265 in catalysis. *Biochemistry* **47**, 9124–35.
- 19 Leferink NGH, Heuts DPHM, Fraaije MW & van Berkel WJH (2008) The growing VAO flavoprotein family. *Arch. Biochem. Biophys.* **474**, 292–301.






- 20 Macheroux P, Kappes B & Ealick SE (2011) Flavogenomics - a genomic and structural view of flavin-dependent proteins. *FEBS J.* **278**, 2625–34.
- 21 Fraaije MW, van Berkel WJH, Benen JAE, Visser J & Mattevi A (1998) A novel oxidoreductase family sharing a conserved FAD-binding domain. *Trends Biochem. Sci.* **23**, 206–207.
- 22 Zafred D, Nandy A, Pump L, Kahlert H & Keller W (2013) Crystal structure and immunologic characterization of the major grass pollen allergen Phl p 4. *J. Allergy Clin. Immunol.* **132**, 696–703.
- 23 Leferink NGH, Fraaije MW, Joosten H-J, Schaap PJ, Mattevi A & van Berkel WJH (2009) Identification of a gatekeeper residue that prevents dehydrogenases from acting as oxidases. *J. Biol. Chem.* **284**, 4392–7.
- 24 Marchler-Bauer A, Zheng C, Chitsaz F, Derbyshire MK, Geer LY, Geer RC, Gonzales NR, Gwadz M, Hurwitz DI, Lanczycki CJ, Lu F, Lu S, Marchler GH, Song JS, Thanki N, Yamashita RA, Zhang D & Bryant SH (2013) CDD: conserved domains and protein three-dimensional structure. *Nucleic Acids Res.* **41**, D348–52.
- 25 Winkler A, Kutchan TM & Macheroux P (2007) 6-S-cysteinylation of bi-covalently attached FAD in berberine bridge enzyme tunes the redox potential for optimal activity. *J. Biol. Chem.* **282**, 24437–43.
- 26 Wallner S, Dully C, Daniel B & Macheroux P (2012) Berberine bridge enzyme and the family of bicovalent flavoenzymes. In *Flavoproteins: 1* (Hille R, Miller SM, & Palfey B, eds), pp. 1–30. De Gruyter, Berlin.
- 27 Hedstrom L (2002) Serine protease mechanism and specificity. *Chem. Rev.* **102**, 4501–24.
- 28 Lindqvist Y, Brändén CI, Mathews FS & Lederer F (1991) Spinach glycolate oxidase and yeast flavocytochrome b2 are structurally homologous and evolutionarily related enzymes with distinctly different function and flavin mononucleotide binding. *J. Biol. Chem.* **266**, 3198–207.
- 29 Winkler A, Lyskowski A, Riedl S, Puhl M, Kutchan TM, Macheroux P & Gruber K (2008) A concerted mechanism for berberine bridge enzyme. *Nat. Chem. Biol.* **4**, 739–41.
- 30 Heuts DPHM, Scrutton NS, McIntire WS & Fraaije MW (2009) What's in a covalent bond? On the role and formation of covalently bound flavin cofactors. *FEBS J.* **276**, 3405–27.
- 31 Kommoju P, Chen Z, Bruckner RC, Mathews FS & Jorns MS (2011) Probing oxygen activation sites in two flavoprotein oxidases. *Biochemistry* **50**, 5521–5534.
- 32 Winkler A, Motz K, Riedl S, Puhl M, Macheroux P & Gruber K (2009) Structural and mechanistic studies reveal the functional role of bicovalent flavinylation in berberine bridge enzyme. *J. Biol. Chem.* **284**, 19993–20001.
- 33 Wallner S, Winkler A, Riedl S, Dully C, Horvath S, Gruber K & Macheroux P (2012) Catalytic and structural role of a conserved active site histidine in berberine bridge enzyme. *Biochemistry* **51**, 6139–47.

- 34 Colloc'h N, Gabison L, Monard G, Altarsha M, Chiadmi M, Marassio G, Sopkova-de Oliveira Santos J, El Hajji M, Castro B, Abraini JH & Prangé T (2008) Oxygen pressurized X-ray crystallography: probing the dioxygen binding site in cofactorless urate oxidase and implications for its catalytic mechanism. *Biophys. J.* **95**, 2415–22.
- 35 Mattevi A, Fraaije MW, Mozzarelli A, Olivi L, Coda A & van Berkel WJ (1997) Crystal structures and inhibitor binding in the octameric flavoenzyme vanillyl-alcohol oxidase: the shape of the active-site cavity controls substrate specificity. *Structure* **5**, 907–20.
- 36 Heuts DPHM, van Hellemond EW, Janssen DB & Fraaije MW (2007) Discovery, characterization, and kinetic analysis of an alditol oxidase from *Streptomyces coelicolor*. *J. Biol. Chem.* **282**, 20283–91.
- 37 Schreuder HA, Hol WGJ & Drenth J (1988) Molecular modeling reveals the possible importance of a carbonyl oxygen binding pocket for the catalytic mechanism of p-hydroxybenzoate hydroxylase. *J. Biol. Chem.* **263**, 3131–3136.
- 38 Bolognesi M, Ghisla S & Incoccia L (1978) The crystal and molecular structure of two models of catalytic flavo(co)enzyme intermediates. *Acta Crystallogr. Sect. B Struct. Crystallogr. Cryst. Chem.* **34**, 821–828.
- 39 Rosini E, Molla G, Ghisla S & Pollegioni L (2011) On the reaction of D-amino acid oxidase with dioxygen: O₂ diffusion pathways and enhancement of reactivity. *FEBS J.* **278**, 482–92.
- 40 Mizutani H, Miyahara I, Hirotsu K, Nishina Y, Shiga K, Setoyama C & Miura R (2000) Three-dimensional structure of the purple intermediate of porcine kidney D-amino acid oxidase. Optimization of the oxidative half-reaction through alignment of the product with reduced flavin. *J. Biochem.* **128**, 73–81.
- 41 Nakajima Y, Miyahara I, Hirotsu K, Nishina Y, Shiga K, Setoyama C, Tamaoki H & Miura R (2002) Three-dimensional structure of the flavoenzyme acyl-CoA oxidase-II from rat liver, the peroxisomal counterpart of mitochondrial acyl-CoA dehydrogenase. *J. Biochem.* **131**, 365–74.
- 42 Jorns MS, Chen ZW & Mathews FS (2010) Structural characterization of mutations at the oxygen activation site in monomeric sarcosine oxidase. *Biochemistry* **49**, 3631–9.
- 43 Schrittwieser JH, Resch V, Wallner S, Lienhart WD, Sattler JH, Resch J, Macheroux P & Kroutil W (2011) Biocatalytic organic synthesis of optically pure (S)-scoulerine and berbine and benzyloquinoline alkaloids. *J. Org. Chem.* **76**, 6703–14.
- 44 Winkler A, Hartner F, Kutchan TM, Glieder A & Macheroux P (2006) Biochemical evidence that berberine bridge enzyme belongs to a novel family of flavoproteins containing a bi-covalently attached FAD cofactor. *J. Biol. Chem.* **281**, 21276–85.
- 45 Nandy A, Petersen A, Wald M, Suck R, Kahlert H, Weber B, Becker WM, Cromwell O & Fiebig H (2005) Primary structure, recombinant expression, and molecular characterization of Phl p 4, a major allergen of timothy grass (*Phleum pratense*). *Biochem. Biophys. Res. Commun.* **337**, 563–70.

- 46 Stankovich MT, Schopfer LM & Massey V (1978) Determination of glucose oxidase oxidation-reduction potentials and the oxygen reactivity of fully reduced and semiquinoid forms. *J. Biol. Chem.* **253**, 4971–4979.
- 47 Minnaert K (1965) Measurement of the equilibrium constant of the reaction between cytochrome c and cytochrome a. *Biochim. Biophys. Acta* **110**, 42–56.
- 48 Kabsch W (2010) XDS. *Acta Crystallogr. D. Biol. Crystallogr.* **66**, 125–32.
- 49 McCoy AJ, Grosse-Kunstleve RW, Adams PD, Winn MD, Storoni LC & Read RJ (2007) Phaser crystallographic software. *J. Appl. Crystallogr.* **40**, 658–674.
- 50 Adams PD, Afonine P V, Bunkóczi G, Chen VB, Davis IW, Echols N, Headd JJ, Hung L-W, Kapral GJ, Grosse-Kunstleve RW, McCoy AJ, Moriarty NW, Oeffner R, Read RJ, Richardson DC, Richardson JS, Terwilliger TC & Zwart PH (2010) PHENIX: a comprehensive Python-based system for macromolecular structure solution. *Acta Crystallogr. D. Biol. Crystallogr.* **66**, 213–21.
- 51 Emsley P, Lohkamp B, Scott WG & Cowtan K (2010) Features and development of Coot. *Acta Crystallogr. D. Biol. Crystallogr.* **66**, 486–501.
- 52 Mayhew SG (1999) The effects of pH and semiquinone formation on the oxidation-reduction potentials of flavin mononucleotide. A reappraisal. *Eur. J. Biochem.* **265**, 698–702.
- 53 Karplus PA & Diederichs K (2012) Linking crystallographic model and data quality. *Science* **336**, 1030–3.
- 54 Bonivento D, Milczek EM, McDonald GR, Binda C, Holt A, Edmondson DE & Mattevi A (2010) Potentiation of ligand binding through cooperative effects in monoamine oxidase B. *J. Biol. Chem.* **285**, 36849–56.

Tables

Table 1. Kinetic data and redox potentials.

	$k_{\text{red}} [S^{-1}]$	$k_{\text{ox}} [M^{-1} s^{-1}]$	$E_0 [mV]$	Oxygen reactivity motif
BBE wildtype ^a	103 ± 4	$(5 \pm 1) \cdot 10^4$	132 ± 4	163  180
BBE G164A	106 ± 13	60 ± 8	109 ± 3	163  180
BBE V169I	18.5 ± 1.4	98 ± 9	109 ± 2	163  180
BBE G164A V169I	0.04 ± 0.002	50 ± 3	110 ± 3	163  180
Phl p 4 wildtype	55 ± 1^d	1.3 ± 0.1	211 ± 2	147  164

Phl p 4 N158H	108 ± 1^d	2.1 ± 0.4	208 ± 1	147 AGVCPTVGVGGHFAGGGF 164
Phl p 4 I153V	53 ± 3^d	$(7.1 \pm 0.2) \cdot 10^4$	205 ± 4	147 AGVCPTIGVGGNFAGGGF 164
Phl p 4 I153V N158H	85 ± 1^d	$(3.9 \pm 0.6) \cdot 10^4$	203 ± 1	147 AGVCPTIGVGGHFAGGGF 164
Free FADH ₂ /FAD	/	250^b	-209^c	
O ₂ /H ₂ O ₂	/	/	270^c	

^a Kinetic data taken from Winkler et al. [25].

^b Data taken from Massey [4].

^c Data taken from Mayhew [52].

^d k_{obs} at 1 mM glucose concentration.

Table 2. Data collection and refinement statistics.

PDB ID	4PVE	4PVH	4PVJ	4PVK	4PWB	4PWC	4PZF
Protein variant	Phl p 4 wildtype	Phl p 4 N158H	Phl p 4 I153V	Phl p 4 I153V N158H	Phl p 4 I153V Xenon pressurized	Phl p 4 I153V N158H 3.5 M NaBr	BBE G164A
Space group	P 6 ₁ 2 2	P 6 ₁ 2 2	P 6 ₁ 2 2	P 6 ₁ 2 2	P 6 ₁ 2 2	P 6 ₁ 2 2	P 2 2 2 ₁
a/b/c (Å)	117.2/117.2/201.5	118.0/118.0/201.1	117.7/117.7/201.7	117.4/117.4/201.0	117.6/117.6/203.0	117.2/117.2/201.5	80.8/175.4/195.8
Mol. in asym. unit	1	1	1	1	1	1	4
Data collection							
(outer shell)							
Wavelength (Å)	1.033	0.980	0.92	0.915	0.92	0.915	0.972
Resolution (Å)	49.2-1.5 (1.554-1.5)	40.7-1.4 (1.450-1.4)	49.4-1.8 (1.864-1.8)	49.3-1.3 (1.346-1.3)	49.4-1.9 (1.968-1.9)	29.3-2.3 (2.382-2.3)	47.4-2.2 (2.279-2.2)
Unique reflections	130268 (12827)	159566 (15565)	76838 (7555)	197673 (18761)	65841 (6459)	37013 (3605)	140140 (13780)
Completeness (%)	100 (100)	98.7 (97.7)	100 (99.9)	99.4 (95.7)	100 (100)	100 (99.9)	98.9 (98.2)
Redundancy	19.6 (19.7)	4.3 (4.2)	19.6 (18.9)	17.4 (7.6)	78.6 (77.2)	39.4 (41.2)	8.3 (8.2)

R _{SYM} (%)	0.12 (1.8)	0.085 (1.5)	0.28 (2.9)	0.090 (2.2)	0.38 (5.4)	0.35 (3.1)	0.12 (1.1)
CC _{1/2} ^a	1.0 (0.76)	1.0 (0.42)	1.0 (0.54)	1.0 (0.27)	1.0 (0.69)	1.0 (0.79)	1.0 (0.79)
Mean I/σ(I)	16.8 (1.7)	11.8 (1.1)	13.0 (1.0)	18.58 (0.71)	26.6 (1.6)	24.9 (2.0)	11.8 (1.52)
Refinement							
R _{WORK} /R _{FREE}	0.133/0.154	0.146/0.167	0.152/0.186	0.141/0.160	0.160/0.187	0.186/0.225	0.220/0.242
Protein atoms	3852	3854	3851	3853	3851	3853	15713
Water atoms	620	700	508	601	377	150	308
Bond length dev. (Å)	0.009	0.009	0.011	0.008	1.34	0.008	0.004
Bond angles dev. (°)	1.32	1.35	1.33	1.32	0.012	1.19	0.84
Clash score	1.78	2.01	1.78	1.39	1.91	5.11	3.38
 protein (Å ²)	20.4	17.8	23.9	19.5	24.4	48.5	54.1
 water (Å ²)	34.1	33.4	35.0	32.5	35.1	46.3	44.2
φ,ψ favoured (%) ^b	96	96	96	96	96	96	95
φ,ψ outliers (%) ^b	0	0	0	0	0	0	0.5

^a CC_{1/2} is the correlation between two halves of a data set, as defined by Karplus and Diederichs [53].

^b Calculated with Phenix [50].

Table 3. Summary of kinetic parameters of BBE variants.

BBE variant	k_{red} [s ⁻¹]	k_{ox} [M ⁻¹ s ⁻¹]	k_{cat} [s ⁻¹]	E ₀ [mV]
wildtype ^a	103 ± 4	(5 ± 1)·10 ⁴	8.0 ± 0.2	132 ± 4
C166A ^a	0.28 ± 0.02	(10 ± 1)·10 ⁴	0.48 ± 0.05	53 ± 2
H104A ^b	3.4 ± 0.3	(8 ± 1)·10 ⁴	0.54 ± 0.02	28 ± 4
H174N ^e	3.0 ± 0.5	(4.1 ± 1.7)·10 ⁴	1.2 ± 0.1	75 ± 3
H174A ^c	0.08 ± 0.01	(7.0 ± 0.3)·10 ³	0.07 ± 0.01	44 ± 3
H459A ^d	88 ± 4	(2.9 ± 0.3)·10 ⁴	3.1 ± 0.7	<i>n.d.</i>
Y106F ^d	6.7 ± 0.6	(3.2 ± 0.3)·10 ⁴	0.7 ± 0.1	<i>n.d.</i>

This article is protected by copyright. All rights reserved.

E417Q ^d	0.067 ± 0.007	(5.3 ± 0.2)·10 ⁴	0.054 ± 0.006	<i>n.d.</i>
G164A ^e	106 ± 13	60 ± 8	0.02 ± 0.002	109 ± 2
V169I ^e	18.5 ± 1.4	98 ± 9	0.02 ± 0.005	109 ± 3
G164A V169I ^e	0.04 ± 0.002	50 ± 3	0.007 ± 0.001	110 ± 3

^a Kinetic data taken from Winkler et al. [25].

^b Kinetic data taken from Winkler et al. [32].

^c Kinetic data taken from Wallner et al. [33].

^d Kinetic data taken from Winkler et al. [29].

^e New data published in this paper.

Table 4. Distances between the reactive C(4a) and the closest side chain atom (or Cα) of the gatekeeper residues for various enzymes from the VAO superfamily.

Protein	BBE	BBE G164A	Phl p 4	Phl p 4 I153V	VAO	AldO
PDB ID	3D2H	4PZF	4PVE	4PVJ	1VAO	2VFR
Oxygen reactivity	oxidase	dehydrogenase	dehydrogenase	oxidase	oxidase	oxidase
Gatekeeper, distance (Å)	Gly (4.7)	Ala (3.7)	Gly (4.5)	Gly (4.7)	Pro (4.4)	Ala (4.1)
Alternate gatekeeper (Å)	Val (4.9)	Val (5.2)	Ile (3.3)	Val (4.7)	N/A*	Ile (5.1)

* There is no residue in the VAO placed at a spatial position analogous to the alternate gatekeeper.

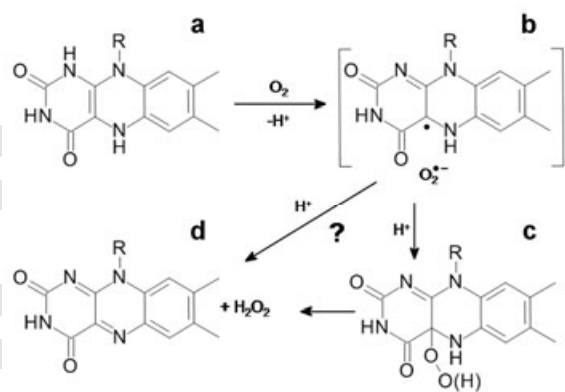


Fig. 1. Oxidative half-reaction of flavoenzyme oxidases.

First electron transfer in the reaction of a reduced FAD (a) with an oxygen molecule is the rate limiting step that yields a radical pair (b) [4]. The pair might form a covalent bond to produce hydroperoxy adduct (c), the intermediate found in monooxygenases that has an sp^3 hybridized C(4a) atom, and subsequent elimination of the hydrogen peroxide yields oxidized FAD (d). Alternatively, the second electron transfer might take place without a bond formation [4].

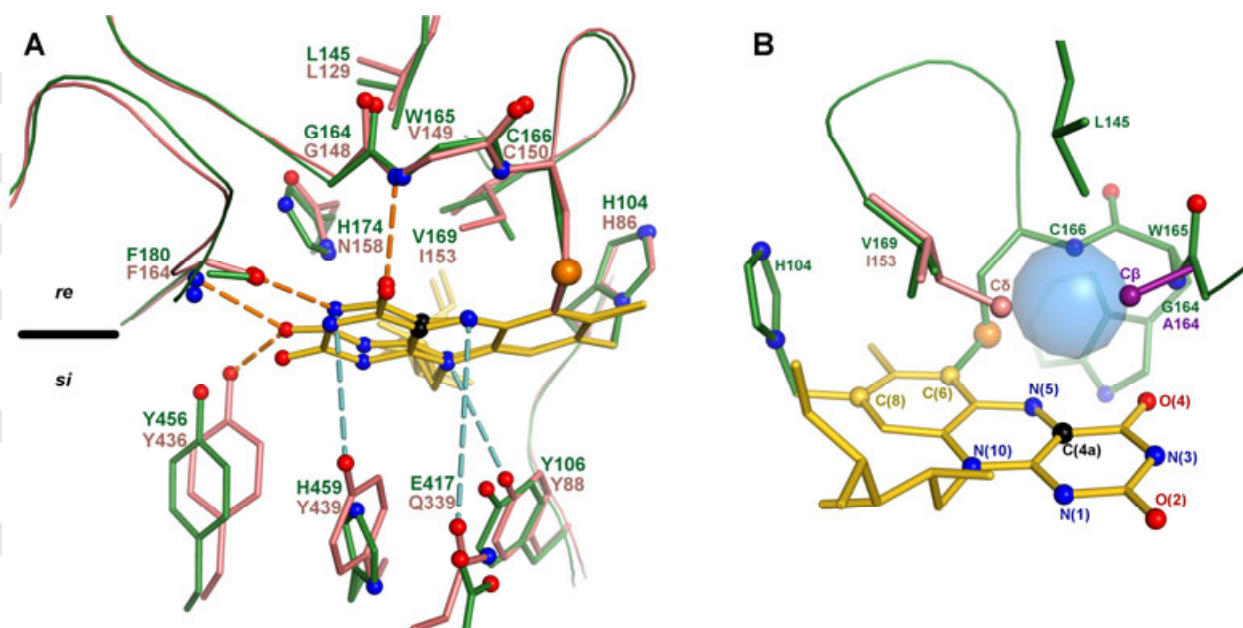


Fig. 2. BBE and Phl p 4 active sites.

(A) Aligned structures of wildtype BBE (green, **PDB ID: 3D2H**) and Phl p 4 (**PDB ID: 4PVE**, pink) in the proximity of FAD (yellow). Three atoms from the isoalloxazine ring are used for the 3D alignment of proteins throughout this paper (C(6), C(8) and N(10)). Hydrogen bonds between flavin and protein matrix are in orange, larger distances that correspond to weak interactions are in blue. The active sites are well conserved, with important exceptions: V169/I153 & H174/N158 on the *re*-face of the isoalloxazine ring and H459/Y439 & E417/Q339 on the substrate binding *si*-face. (B) A view of the *re*-face of the FAD in wildtype BBE where a cavity (blue sphere) forms the oxygen pocket together with the backbone nitrogen atoms of C166 and W165, the proposed proton donors. BBE G164A variant (**PDB ID: 4PZF**, purple) and Phl p 4 (pink) are aligned to show how side chains of the alternate gatekeeper I169/I153 and the gatekeeper A164 extinguish the cavity by pointing towards the reactive C(4a) carbon atom (black).

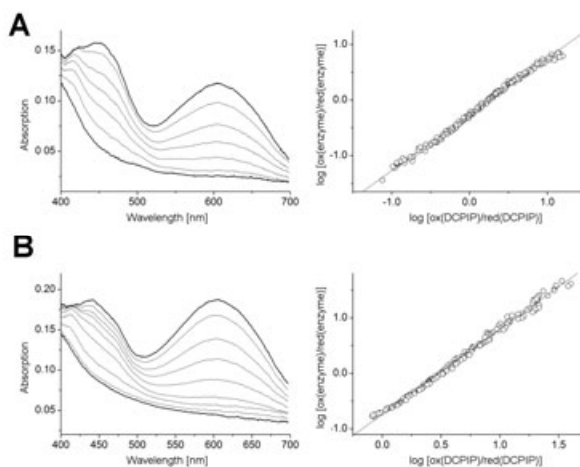


Fig. 3. Redox potential determination.

Plots of the selected spectra of the course of reduction are shown for wildtype Phl p 4 (A) and the double mutant Phl p 4 I153V N158H (B). The double logarithmic plots were used in the evaluation of data according to Minnaert [47].

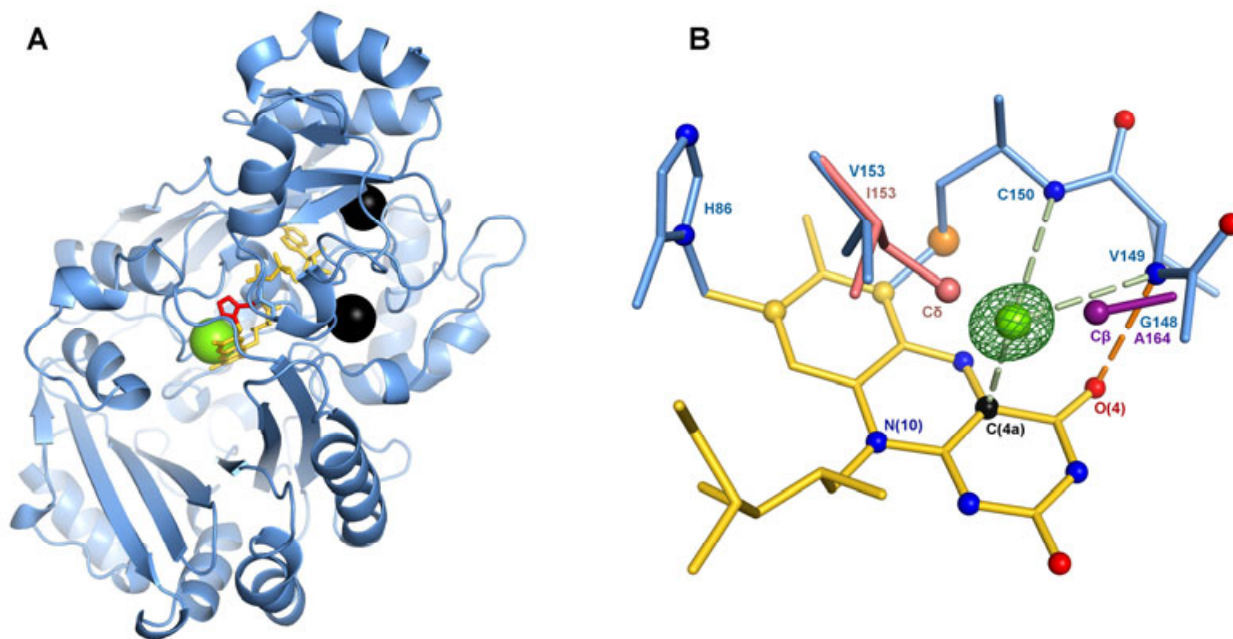


Fig. 4. Structures with oxygen surrogates.

(A) Cartoon representation of Phl p 4 I153V variant (**PDB ID: 4PWB**) with FAD (yellow) in stick representation and the H86 in red for easier orientation. The substrate binding site is formed by a large cavity below the flavin ring (*si*-face). Xenon atoms are presented as black spheres and a bromide ion, shown in green at the *re*-face of the FAD, is aligned from the bromide soak structure (Table 2). (B) Phl p 4 I153V N158H variant (**PDB ID: 4PWC**, blue) accommodates a bromide in the oxygen pocket. The oxygen surrogate placed into the difference omit map (green mesh) is positioned 2.5 Å above the reactive C(4a) (black atom in yellow FAD) and 3.4 Å from backbone nitrogen atoms of C150 and V149, the latter is in a hydrogen bond distance with the carbonyl O(4) (orange). In our structures, the ion is only 1.5 Å and 1.7 Å from the side chains of I153 and A164 in aligned wildtype Phl p 4 (**PDB ID: 4PVE**, pink) and BBE G164A (**PDB ID: 4PZF**, purple), respectively.

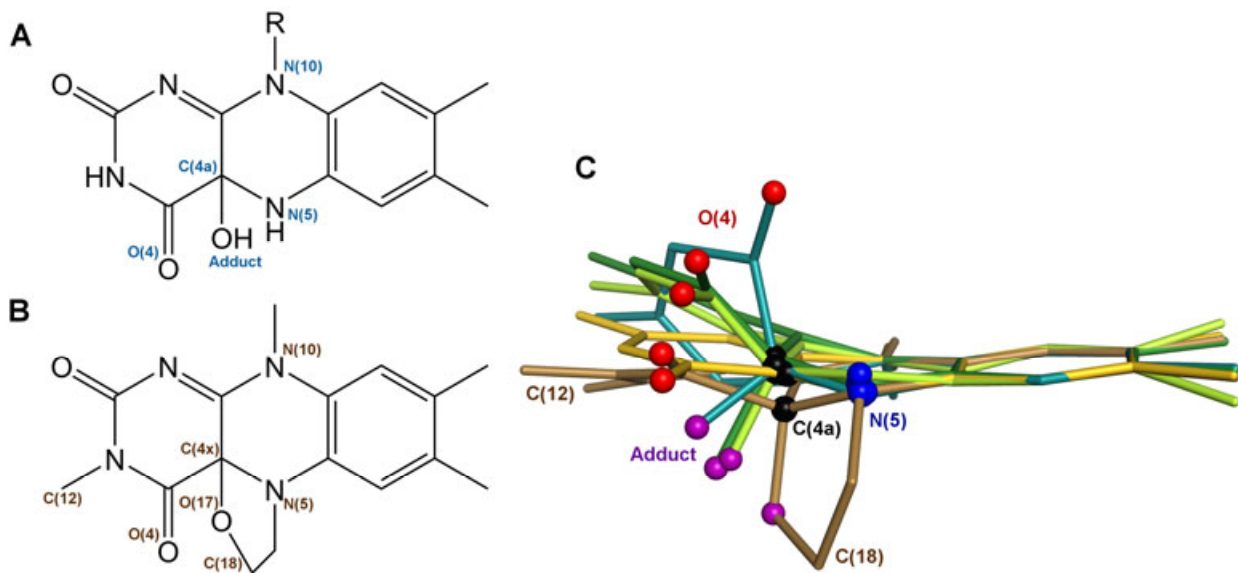


Fig. 5. Four flavin derivatives used for models of putative C(4a) adduct intermediate states.

(A) Flavin derivative from crystal structure of choline oxidase (**PDB ID: 2JBV**) with oxygen adduct placed at the position at which authors assigned an “unknown atom” [10]. (B) Drawing of the 4a,5-epoxyethano-3-methyl-4a,5-dihydroflavin (Emmdh-flavin) [38]. The position of C(18) was used in our models of hydroperoxy flavins for placing the distal oxygen atom in a proposed orientation relative to the N(5). (C) 3D alignment of structures of flavin derivatives shows that orientation of the adduct and movement of the carbonyl C(4)=O out of the plane may vary significantly. FAD from a PhI p 4 structure is yellow, Emmdh-flavin is brown and three derivatives are from protein X-ray structures: pyranose dehydrogenase (**PDB ID: 4H7U**, light green) [11], human monoamine oxidase B (**PDB ID: 2XCG**, dark green) [54] and choline oxidase (**PDB ID: 2JBV**, cyan) [10].

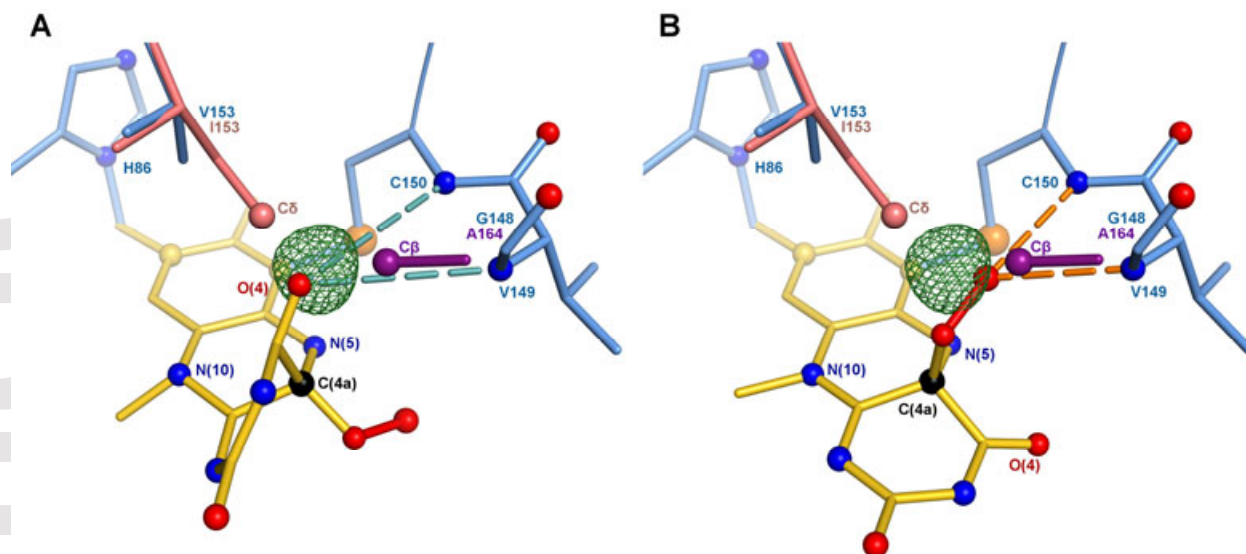


Fig. 6. Models of putative intermediates placed in Phl p 4.

Models of flavin derivative are placed in the structure of Phl p 4 I153V N158H bromide soak (**PDB ID: 4PWC**, blue) and position of the bromide ion is shown with its F_o-F_c difference density (green). Structures of wildtype Phl p 4 (pink) and BBE G164A (purple) are aligned and represented by the gatekeeper residues. (A) Model based on the derivative structure from choline oxidase (**PDB ID: 2JBV**) with C(4a) hydroperoxy adduct on its *si*-face shows that C(4)=O oxygen atom can freely move into the oxygen pocket in wildtype BBE and in Phl p 4 I153V variants. Blue lines represent distances larger than 3.5 Å. (B) Model based on the structure of Emmdh-flavin with C(4a) hydroperoxy adduct on its *re*-face shows that the adduct fits into the oxygen pocket where it can form hydrogen bonds (orange) with the backbone nitrogens of C150 and possibly also V149. This intermediate cannot form in BBE G164A variant due to a clash with the gatekeeper, nor can it form in wildtype Phl p 4 or BBE V169I due to a clash with C(δ) of the alternate gatekeeper residue I169/I153.

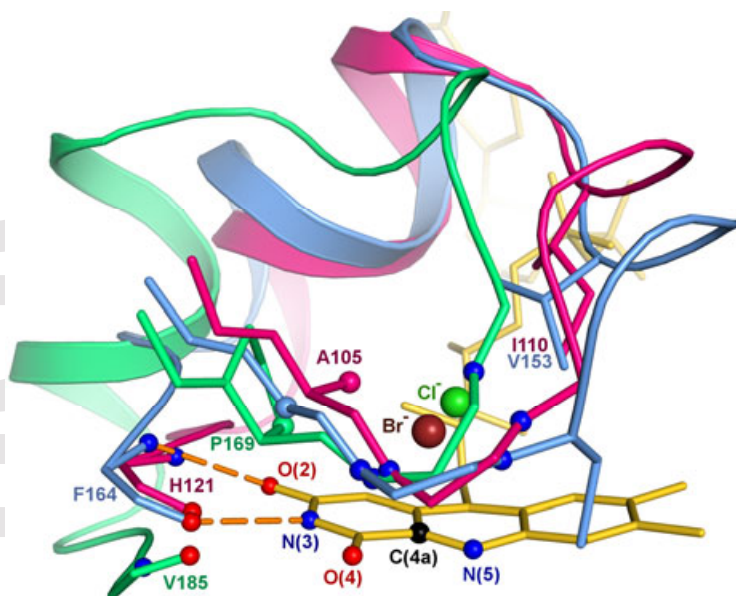


Fig. 7. The oxygen reactivity motif.

The motif defining dioxygen reactivity in VAO enzymes is shown in aligned structures of Phl p 4 I153V N158H bromide soak (**PDB ID: 4PWC**, blue), VAO (**PDB ID: 1VAO**, green) and AldO (**PDB ID: 2VFR**, purple). Position of the gatekeeper residues G148/P169/A105 and the position of the first proton donor backbone nitrogen (blue spheres above O(4)) are highly conserved. The rest of the backbone is less aligned which influences the spatial position and size of the oxygen pocket, represented here by the bromide (brown) and chloride (green) anions that reside in the cavities of Phl p 4 and VAO, respectively. The motif ends in residues F164/V185/H121 which form two strong and conserved hydrogen bonds (shown for Phl p 4 in orange) with N(3) and O(2) through their backbone oxygen and nitrogen atoms.

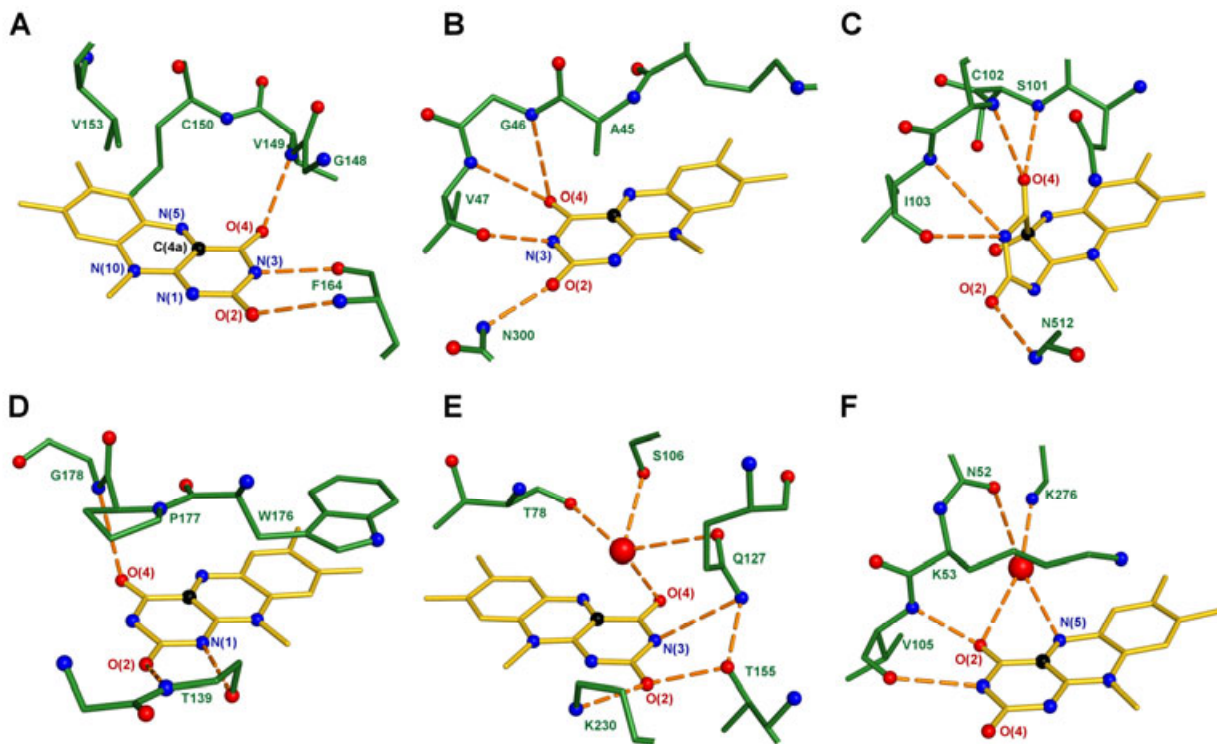


Fig. 8. Flavoenzyme oxidases from various structural superfamilies.

At the first glance, environments of FAD in Phl p 4 (PDB ID: 4PVE, A) and PHBH (PDB ID: 1PHH, B) look as if they were mirror images. The putative oxygen pocket accommodates C(4)=O carbonyl atom of FAD in the structure of choline oxidase (PDB ID: 2JBV, C) which, like PHBH, belongs to the GMC structural superfamily. Peroxisomal acyl-CoA oxidase (PDB ID: 1IS2, D) belongs to the acyl-CoA dehydrogenase superfamily and has a putative oxygen pocket at the *si*-face of the FAD where backbone nitrogens of P177 and G178 reside. The proposed oxygen pocket in glycolate oxidase (PDB ID: 1GOX, E) that belongs to the superfamily of FMN-linked oxidoreductases is formed by the side chains of S106 and Q127 and is filled with a water molecule in the native crystal [28]. A strongly bound water molecule is also found in fructosamine oxidase (PDB ID: 3DJE, F) where the proton donors of the oxygen pocket could be the water molecule and the backbone nitrogen of V105.